

Hydrogen Adsorption in MOF-74 Studied by Inelastic Neutron Scattering

Yun Liu^{1,2}, Craig M. Brown¹, Dan A. Neumann¹, Houria Kabbour³, and Channing C. Ahn³

¹NIST Center for Neutron Research, 100 Bureau Drive, MS6102, Gaithersburg, MD, 20899

²Department of Materials Science and Engineering, University of Maryland, College Park, MD, 20742

³Division of Engineering and Applied Science, California Institute of Technology, Pasadena, CA, 91125

ABSTRACT

Adsorption of hydrogen and the occupancy of different binding sites as a function of hydrogen loading in MOF-74 are studied using inelastic neutron scattering (INS). Hydrogen molecules are observed to fully occupy the strongest binding site before populating other adsorption sites. The comparison of the INS spectra at 4 K and 60 K indicates that hydrogen adsorbed at the strongest binding site is strongly bound and localized. We also show that when two hydrogen molecules are adsorbed into a single, attractive potential well, the shortest inter-H₂ distance is about 3 Å, consistent with our previous observation of inter-H₂ distance when adsorbed in two neighboring potential wells.

INTRODUCTION

Adsorbing H₂ in nano-porous materials with large surface areas has attracted significant attention in past years. It has been shown for activated carbons that about 1 wt% of hydrogen can be adsorbed for every 500 m²/g of surface area. [1] This has been a strong impetus in striving to increase material surface areas and achieve a concomitant increase in hydrogen uptake. For example, it has been reported that MOF-177 has N₂ Brauner-Emmett-Teller (BET) surface area of 4746 m²/g; [2] and some carbon aerogels can have N₂ BET surface areas of \approx 3200 m²/g. [3] The saturation excess adsorption (SEA) at 77 K is \approx 7.5 wt% for MOF-177 [2] and \approx 5.3 wt% for carbon aerogel. [3] However, due to the generally low binding strength of hydrogen, the SEA value decreases dramatically with increasing temperature. It has been shown in the cases of a few metal-organic framework (MOF) materials that the coordinately unsaturated metal centers (CUMCs) can greatly enhance the binding strength of H₂ in MOFs. [4-7] Of these examples, the Mn-BTT material has an initial hydrogen adsorption enthalpy of about 10.1 kJ/mol due to the direct interaction between hydrogen molecules and the exposed Mn²⁺ ions. [4] Hence, it is therefore extremely important to understand this hydrogen-CUMCs interaction and direct efforts for optimizing the material synthesis.

MOF-74 has one-dimensional pore channels of size \approx 10 Å. [8-9] Previously, using neutron powder diffraction techniques, we have shown that the relatively large initial hydrogen adsorption enthalpy (about 8.8 kJ/mol) is due to a direct interaction of hydrogen molecules with the open Zn²⁺ ions in the framework. [7] The hydrogen molecules adsorbed on the surface of the pore are packed denser than the molecules in solid hydrogen. We have also shown, using a model system of two hydrogen adsorption sites placed close to each other, that the smallest interaction distance between physisorbed hydrogen molecules under technologically relevant

conditions is only $\approx 3 \text{ \AA}$. [7] However, some issues remain unclear and will be addressed in this paper.

First, we performed site specific INS spectroscopy to understand how the different adsorption sites are occupied as a function of hydrogen loading. Comparison is made to the case of HKUST-1, where the strongest hydrogen adsorption sites are only partially occupied before weaker sites are populated. [10] Second, although we have demonstrated previously that the binding strength of the different sites in MOF-74 is significantly different, we would like to know how mobile the hydrogen molecules are with increasing temperature. This is achieved by comparing the INS spectra obtained at both high temperature and 4 K with exactly the same loading. Thirdly, we shall extend and compliment our previous calculations by looking at a system having a single potential well that is able to attract two hydrogen molecules.

EXPERIMENT

The synthesis and sample activation procedures for MOF-74 ($\text{Zn}_2(\text{C}_8\text{H}_2\text{O}_6)$) are already reported in previous publications. [7-9] Prior to the neutron experiments, the sample was further degassed at $120 \text{ }^\circ\text{C}$ overnight. The sample was then transferred into a vanadium sample can sealed with an indium o-ring and fitted with a valve. All the sample handling/transferring was performed in a helium glove box with oxygen and humidity sensors. The sample can was then mounted on a sample stick with a gas loading line. The gas loading line was first pumped to a good vacuum before opening the valve on the sample can. The sample stick was then put into a top-loading closed-cycle refrigerator (CCR) and cooled to 4 K for measurements.

Hydrogen gas at room temperature is a mixture of 25% para- H_2 and 75% ortho- H_2 . [11] Although the effect of the mixture on hydrogen adsorption properties is not expected to be significantly in most situations, para- H_2 and ortho- H_2 have very large differences in neutron scattering cross sections. [12] In order to make the spectrum relatively simple, we have used a modified CCR with a paramagnetic catalyst to convert the normal hydrogen into predominantly para-hydrogen. Only para- H_2 was used in the experiments reported here.

For each hydrogen loading, the sample was first warmed to $\approx 50 \text{ K}$ and then the calculated amount of H_2 gas was loaded to a container with a known volume at room temperature. The sample was then exposed to the hydrogen gas in the container. After the gas reached equilibrium at 50 K, The temperature was then slowly cooled down to 4 K. The pressure gauge always read zero before the temperature reached 25 K indicating all the hydrogen was adsorbed.

The INS spectra were obtained using the Filter Analyzer Neutron Spectrometer (FANS) at the National Institute of Standards and Technology Center for Neutron Research (NCNR). [13] The pyrolytic graphite monochromator was used with collimation of $20'$ and $20'$ before and after the monochromator, respectively, to produce a collimated, monoenergetic beam of neutrons. The overall energy resolution is about 1.2 meV between 6 meV and 15 meV and degrades with the further increase of energy.

DISCUSSION

Figure 1 shows the typical INS spectra of H_2 adsorbed in MOF-74 with loadings corresponding to 0.2 $\text{H}_2:\text{Zn}$, 0.6 $\text{H}_2:\text{Zn}$, 1.0 $\text{H}_2:\text{Zn}$, 1.2 $\text{H}_2:\text{Zn}$, and 2.0 $\text{H}_2:\text{Zn}$ after subtracting the bare MOF-74 background spectrum. According to our previous work using neutron powder

diffraction, there are 4 adsorption sites for hydrogen in MOF-74, with the first 3 adsorption sites dominating the adsorption properties at 77 K. [7] The first site is termed the ‘Zn site’ since the hydrogen molecule is directly associated with the Zn^{2+} ion. When there is only 0.2 H_2 :Zn in the sample, we would expect that only the Zn site is occupied. Clearly, we can see that there are many peaks in the INS spectrum even when hydrogen molecules are adsorbed at one site. This seems to be a general observation for hydrogen molecules adsorbed in metal-organic frameworks [7,10] and hence, one needs to be careful in assigning peaks to different adsorption sites.

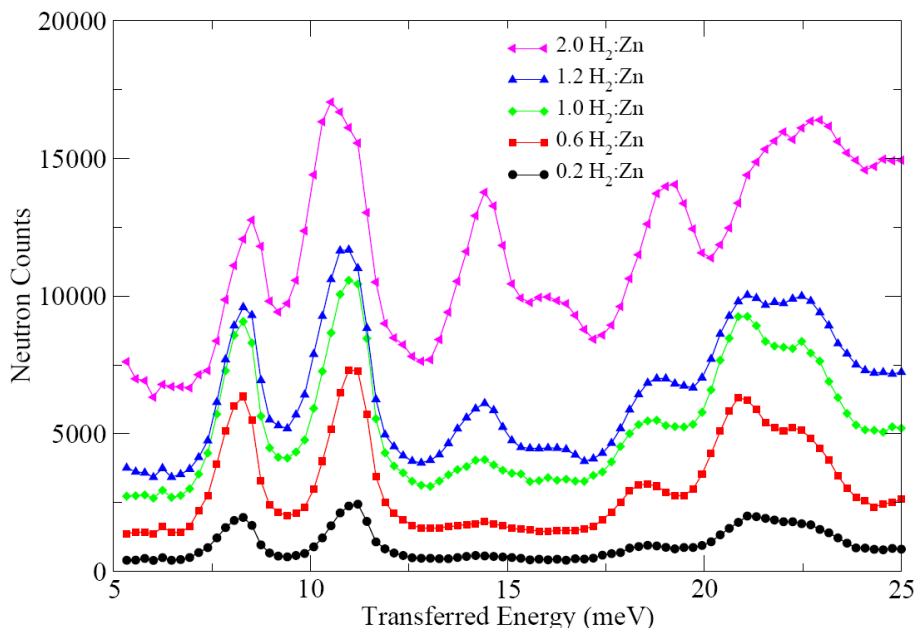


Figure 1. The inelastic neutron scattering spectra of adsorbed H_2 in MOF-74 after subtracting the bare MOF-74 spectrum. Error bars are smaller than the symbols.

H_2 consists of two protons with the spin $\frac{1}{2}$ for each proton. The total wave function of the two fermions needs to be anti-symmetric. When the total spin of H_2 , S , is 0, an H_2 is called para- H_2 and its rotational wavefunction have to be symmetric, i.e., the rotation quantum number, J , needs to be 0, 2, ... [11] When the total spin of the two protons, S , is 1, an H_2 is called ortho- H_2 and the associated J has to be 1, 3, ... For a freely rotating molecule in a three dimensional system, $E = BJ(J+1)$, where E is the rotational eigenenergy and $B = 7.35$ meV, the rotational constant of hydrogen. [11] Due to spin correlation, the neutron scattering cross section for transitions between para- states is very small. [12] On the other hand, the neutron scattering cross section of transitions between para- and ortho- states is very large and usually dominates an INS spectrum. [10, 12] Since we have used para- H_2 in these experiments, the prominent scattering features we observe are mainly due to transitions associated between para- H_2 and ortho- H_2 .

When the spin state of a H_2 is changed, there is corresponding change of its rotational wavefunction, and hence a change of energy. For a freely rotating H_2 , a peak at 14.7 meV is usually observed, which is due to the transition from $J = 0$ to $J = 1$. [11-12] At 4 K, all para- H_2 should be in the rotational ground state, i.e., $J = 0$. Because of the large rotational barrier of hydrogen adsorbed in MOF-74, the $J = 1$ eigenenergy levels are split and coupled with other rotational eigenstates and possibly translational motions, which result in the rich features for hydrogen adsorbed even at one adsorption site. A detailed analysis of the wavefunctions

associated with each peak needs much more calculation, which will be addressed in a future paper. Here we take a phenomenological approach to understand the features of the spectra. Since the scattering cross section for a transition from para- to ortho- H_2 is incoherent in nature, it reflects only the individual molecules. Hence the scattering features are additive. Therefore, by analyzing the intensity of each characteristic peak, we can estimate the amount of hydrogen adsorbed at the different sites.

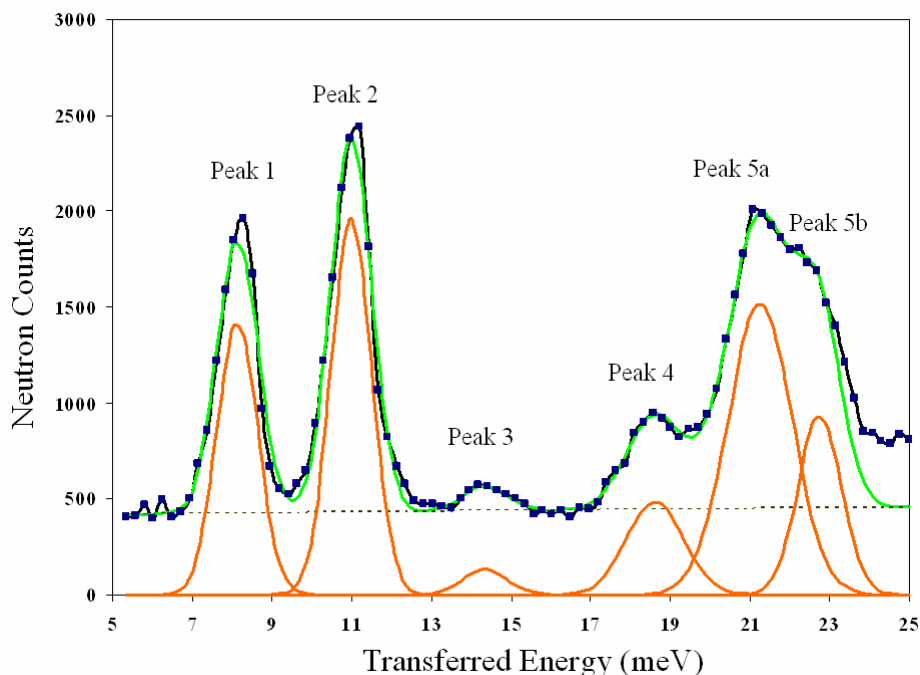


Figure 2. Gaussian peaks are used to fit the spectrum of 0.2 H_2 :Zn loaded MOF-74. A slope function is used to fit the background signal. The FWHM of peak 1 and peak 2 are fixed as 1.2 meV, which is the instrument energy resolution in this energy range.

Figure 2 shows the spectrum for the case of 0.2 H_2 :Zn along with a phenomenological description of the data. A slope function is used to simulate the background signal, which is shown as a dashed line. Each peak is fitted with a Gaussian function. The solid green line is the fitted curve. The full-width at half peak-maximum (FWHM) of peak 1 at $E \approx 8.1$ meV and peak 2 at $E \approx 10.9$ meV is resolution limited and during the fitting the FWHM was fixed as 1.2 meV. Peak 1 and 2 are tentatively assigned to the rotational transitions associated with para- to ortho- H_2 transitions. The origin of peak 3, 4, 5 is difficult to be assigned without further measurements. Currently, we speculate that peak 3 may be due to the rotational translation coupling. Peak 5 contains at least two peaks and we used two Gaussian peaks (peak 5a and peak 5b) to fit it. One of them could be due to a rotational transition. The rotational peak splitting observed for H_2 adsorbed on single-walled carbon nanotubes or C_{60} , is only ≈ 1 meV. [14-17] The large rotational splitting observed here would be on the order of 10 meV, indicative of the much larger rotational barrier generated by the metal-organic framework. This picture is consistent with observation of H_2 adsorbed in HKUST-1. [10] When the amount of adsorbed hydrogen is larger than 1.0 H_2 :Zn, peak 2 becomes broad and peak 3's intensity increases. Both peak 2 and 3 have to be fitted with multiple Gaussian peaks. This indicates that hydrogen molecules are adsorbed at

different sites which have different rotational barriers, giving rise to the more complicated spectrum spectrum.

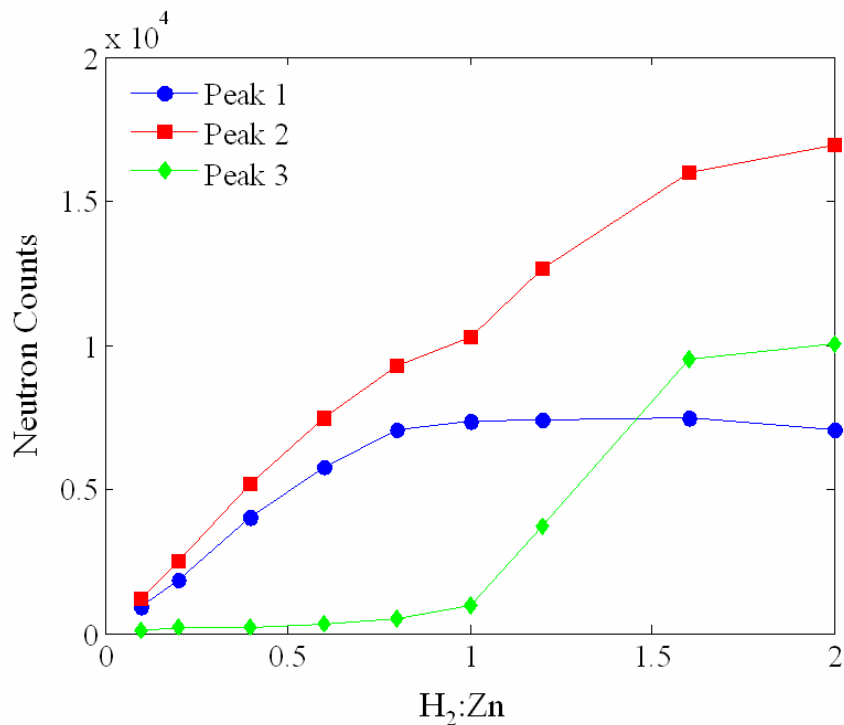


Figure 3. The variation of peak areas as a function of H₂ loading. The peak areas are obtained by fitting the peaks with one or two Gaussian functions. Peak 1 is a characteristic peak for H₂ adsorbed at site 1.

Figure 3 plots the neutron counts under each peak obtained by fitting the spectra as a function of adsorbed hydrogen. Peak 1 is a characteristic peak for the Zn site only. It saturates at ≈ 1.0 H₂:Zn. Peak 2 increases initially and begins to plateau at ≈ 1.0 H₂:Zn before the slope increases with further H₂ loading. This indicates that peak 2 is a characteristic feature of the Zn site at low loadings smaller than 1.0 H₂:Zn. When the Zn site is saturated, other sites begin to be populated causing the broadening and the increase in intensity of peak 2. This increase is mirrored with the change of intensity of peak 3. Initially, the intensity of peak 3 is very small. When the amount of adsorbed hydrogen is larger than 1.0 H₂:Zn, the intensity of peak 3 increases indicating that there are strong rotational transitions just under 15 meV due to population of sites other than the Zn site. We can therefore surmise that in MOF-74, the Zn site is first fully populated before other weaker binding sites are occupied. This is in contrast to what we observed in the case of HKUST-1, where the weaker binding sites are populated before the strongest binding site is fully occupied. [10] The possible reason for this behavior is that the binding energy difference between the first and subsequent sites in MOF-74 is much larger than that in HKUST-1.

Due to the strong binding of H₂ at the Zn site, H₂ molecules should not move too much even at high temperature. Figure 4 shows the INS spectra of H₂ adsorbed at the Zn site obtained at 4 K and 60 K. The sample was loaded with about 2.8 H₂:Zn and subsequently degassed for

approximately 30 minutes at 60 K. After this time, we measured the INS spectra at both 4 K and 60 K. From comparison to the previously loaded data, we can estimate the amount of hydrogen as $\approx 0.6 \text{ H}_2/\text{Zn}$ remaining after the degassing procedure. Comparing peak 1 and 2 at both temperatures, there is only a slight broadening indicating that the hydrogen molecules at the Zn sites are very strongly bound even at 60 K. The absence of any significant intensity at peak 3 indicates that the hydrogen molecules adsorbed at site 2 and site 3 are not so strongly bound that they can be removed at 60 K. Nevertheless, these sites can still be populated at 77 K when pressures are applied.

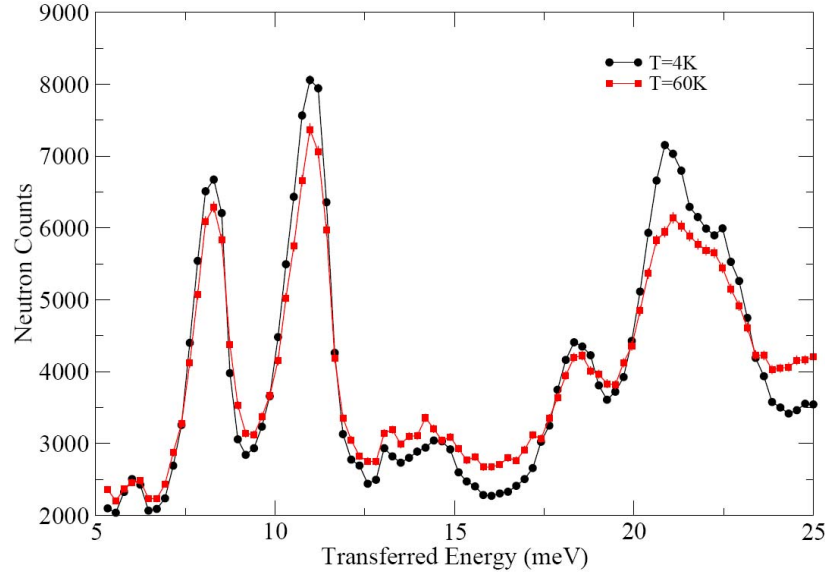


Figure 4. The comparison of the INS spectra of H_2 adsorbed in MOF-74 at 4 K and 60 K. Error bars are smaller than the symbols.

In the previous paper [7], we have estimated that for physisorbed hydrogen molecules pulled close to each other using strong attractive harmonic potentials, the smallest distance obtainable between two H_2 molecules is around 3.0 \AA . However, sometimes, one harmonic potential may also hold multiple hydrogen molecules. Therefore, it is interesting to understand how close hydrogen molecules can approach each other under this situation. Two hydrogen molecules are put into a wide square well potential. A harmonic potential is then added, which is defined as

$$V_h(r) = \begin{cases} \frac{1}{2} m \omega^2 r^2 - E_d & \text{if } \frac{1}{2} m \omega^2 r^2 < E_d \\ 0 & \text{if } \frac{1}{2} m \omega^2 r^2 > E_d \end{cases}$$

where E_d is the potential depth and $\hbar\omega$ is the quantized energy difference between neighboring eigenenergy levels for a harmonic potential, m is the molecular mass of a hydrogen molecule. The inter- H_2 potential is taken from reference [11]. The average distance between the two hydrogen molecules, r_{HH} , is then calculated. The detailed calculation method is described elsewhere. [7]

The results are shown in Figure 5 upon changing the potential depth, E_d , and $\hbar\omega$. When $E_d = 0 \text{ meV}$, r_{HH} is $\approx 4.9 \text{ \AA}$. In general, with the increase of potential depth, r_{HH} decreases. At $\hbar\omega = 2 \text{ meV}$, r_{HH} first decreases to a plateau at $\approx 4.58 \text{ \AA}$ at $E_d = 10 \text{ meV}$, where only one H_2 molecule

is held by the attraction potential and becomes less mobile. With a slight further increase of E_d , r_{HH} plummets to about 3.53 \AA at $E_d = 15 \text{ meV}$ because the potential well becomes wide enough for two H_2 molecules to be simultaneously accommodated. Once both H_2 molecules are attracted by the potential well, r_{HH} changes little with increasing E_d .

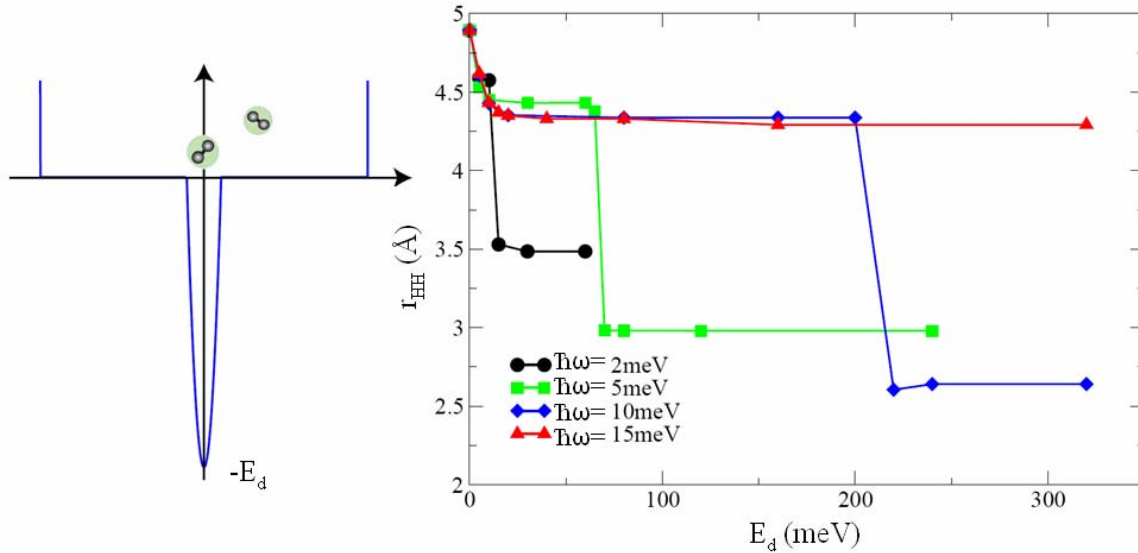


Figure 5. The calculation of the distance between two hydrogen molecules phisorbed by one harmonic potential.

In order to move the H_2 molecules even closer, we have tested cases where $\hbar\omega = 5 \text{ meV}$, 10 meV , and 15 meV . With the increase of E_d , r_{HH} reaches a first plateau of about 4.4 \AA , 4.3 \AA , and 4.3 \AA respectively. Larger $\hbar\omega$, indicating a steeper change of the potential well, results in a smaller r_{HH} . The relatively large r_{HH} shows that when only one H_2 is tightly bound to the attractive potential, the second H_2 can not approach very closely. With further increase of the potential depth, r_{HH} plunges to a second plateau with a value of r_{HH} about 2.94 \AA for $\hbar\omega = 5 \text{ meV}$ and 2.6 \AA for $\hbar\omega = 10 \text{ meV}$ when both H_2 are attracted. Once both H_2 molecules are in the potential well, an increase of $\hbar\omega$ decreases r_{HH} . Due to the strong repulsion between H_2 molecules, for a given $\hbar\omega$, E_d has to be large enough to hold both molecules inside the potential. There is no second plateau for $\hbar\omega = 15 \text{ meV}$ with potential depth up to 320 meV although we expect r_{HH} to reach a second plateau if the potential depth is further increased.

The results show that in order to bind H_2 molecules close to each other, a stronger binding potential is always necessary. Once both molecules are bound in a single potential, the steepness of the potential wall will eventually determine the equilibrium distance between H_2 molecules. We notice that the potential depth needed to bind two H_2 molecules is not too large. For $\hbar\omega = 5 \text{ meV}$, E_d only needs to be about 70 meV , which is readily reachable by most carbon based materials. In reality, the potential shape differs from a harmonic potential. The change of r_{HH} as a function of E_d may be smoother than that of the current case. When temperature is a factor, for instance at 77 K , the thermal energy of a H_2 molecule is about 6.6 meV , which will affect the result of the second plateau when $\hbar\omega = 2 \text{ meV}$. For this case, a larger E_d will be needed to bind both H_2 molecules at 77 K . However, the results for $\hbar\omega = 5 \text{ meV}$, 10 meV , and 15 meV

are expected to be less affected. The minimum inter-H₂ distance can reach about 2.6 Å when E_d is very large. For most carbon based materials, the surface could not provide such a strong potential, hence, the minimum distance that could realistically be achieved upon a carbon surface is only about 3 Å.

CONCLUSIONS

Hydrogen molecules adsorbed in MOF-74 have been studied using inelastic neutron scattering. By analyzing the different peak intensities due to hydrogen molecules adsorbed at different sites, the occupancy number at those sites are estimated as a function of adsorbed hydrogen. H₂ is observed to completely saturate the first site before populating other sites, which is attributed to the large binding energy difference between the first adsorption site and other sites in MOF-74. The comparison of spectra obtained at 4 K and 60 K show that the first binding site strongly binds hydrogen even at 60 K. The estimation of the minimum hydrogen molecule distance based on surface adsorption is estimated to be around 3 Å, consistent with the results in our previous calculations and comparable to what we have previously measured using neutron diffraction.

ACKNOWLEDGMENTS

The authors wish to thank J. Leão and S. Slifer for experiment assistance and M. A. Green for useful discussion. This work was partially supported by the U. S. Department of Energy's Office of Energy Efficiency and Renewable Energy within the Hydrogen Sorption Center of Excellence.

REFERENCES

1. R. Chahine, P. Benard, In *Advance in cryogenic engineering*; Kittel, P., Ed.; Plenum Press: New York, 1998; Vol. 34, p 1257.
2. A. G. Wong-Foy, A. J. Matzger, O. M. Yaghi, *J. Am. Chem. Soc.* **128**, 3494-3495 (2006).
3. H. Kabbour, T. F. Baumann, J. H. Satcher, Jr., A. Saulnier, C. C. Ahn, *Chem. Mater.* **18**, 6085-6087 (2006).
4. M. Dincă, A. Dailly, Y. Liu, C. M. Brown, D. A. Neumann, J. R. Long, *J. Am. Chem. Soc.* **128**, 16876-16883 (2006).
5. M. Dincă, W. S. Han, Y. Liu, A. Dailly, C. M. Brown, J. R. Long, *Angew. Chem. Int. Ed.* **46**, 1419-1422 (2007).
6. V. K. Peterson, Y. Liu, C. M. Brown, C. J. Kepert, *J. Am. Chem. Soc.* **128**, 15578-15579 (2006).
7. Y. Liu, H. Kabbour, C. M. Brown, D. A. Neumann, C. C. Ahn, submitted (2007).
8. N. L. Rosi, J. Kim, M. Eddaoudi, B. Chen, M. O'Keeffe, O. M. Yaghi, *J. Am. Chem. Soc.* **127**, 1504-1518 (2005).
9. Rowsell, J. L. C., Yaghi, O. M. *J. Am. Chem. Soc.* **128**, 1304-1315 (2006).
10. Y. Liu, C. M. Brown, D. A. Neumann, V. K. Peterson, C. Kepert, *J. of Alloys and Compounds* **446-447**, 385 (2007).
11. I. F. Silvera, *Rev. Mod. Phys.* **52**, 393-452 (1980).
12. J. A. Young, J. U. Koppel, *Phys. Rev.* **135**, A603, (1964).

13. T. J. Udovic, D. A. Neumann, J. Leao, C. M. Brown, *Instrum. Methods* **A517**, 189 (2004).
14. C. M. Brown et al., *Chem. Phys. Lett.* **329**, 311 (2003).
15. Y. Liu et al. *J. of Alloys and Compounds* **446-447**, 368 (2007).
16. S. A. FitzGerald et al., *Phys. Rev. B* **60**, 6439 (1999).